

Pulse mode shear horizontal-surface acoustic wave (SH-SAW) system for liquid based sensing applications

Fabrice Martin^a, Michael I. Newton^{a,*}, Glen McHale^a,
Kathryn A. Melzak^b, Electra Gizeli^b

^a School of Science, The Nottingham Trent University, Clifton Lane, Nottingham NG11 8NS, UK

^b Institute of Biotechnology, University of Cambridge, Tennis Court Road, Cambridge CB2 1QT, UK

Received 30 October 2002; received in revised form 27 June 2003; accepted 9 July 2003

Abstract

In this work, we describe a novel pulse mode shear horizontal-surface acoustic wave (SH-SAW) polymer coated biosensor that monitors rapid changes in both amplitude and phase. The SH-SAW sensors were fabricated on 36° rotated Y-cut X propagating lithium tantalate (36 YX.LT). The sensitivity of the device to both mass loading and visco-elastic effects may be increased by using a thin guiding layer of cross-linked polymer. Two acoustic modes are excited by the electrodes in this crystalline direction. Metallisation of the propagation path of the 36 YX.LT devices allows the two modes to be discriminated. Successive polymer coatings resulted in the observation of resonant conditions in both modes as the layer thickness was increased. Using the 36 YX.LT devices, we have investigated the application of a novel pulse mode system by sensing a sequence of deposition and removal of a biological layer consisting of vesicles of the phospholipid POPC. A continuous wave system was used to verify the accuracy of the pulse mode system by sensing a series of poly(ethylene glycol) (PEG) solutions. The data clearly demonstrates the ability of the 36 YX.LT pulse mode system to provide rapid measurements of both amplitude and phase for biosensing applications.

© 2003 Elsevier B.V. All rights reserved.

Keywords: Acoustic wave; SH-SAW; SSBW; Love wave; Biosensor

1. Introduction

Acoustic sensors based on shear-horizontal (SH) waves have become popular in recent years due to their ability to operate in liquid media. Love waves are guided SH acoustic modes that propagate in a thin layer deposited on top of a substrate (Gulyaev, 1998). The acoustic energy is concentrated in this guiding layer, which leads to an increased mass sensitivity. To eliminate the influence of the electric properties of an adjacent liquid, a metallisation can be applied on top of the guiding layer. Love-wave devices incorporating guiding layers of spun polymethylmethacrylate (PMMA) on ST-Quartz were first reported for biosensing applications by Gizeli et al. (1992). The use of sputtered SiO₂ as an alternative overlayer material was reported by Kovacs et al. (1994) and this was extended to use chemical vapor deposition of the SiO₂ by Jakob and Vellekoop (1998); the use of multi-

layer Love-wave structures has also been reported (Harding and Du, 1997; Du and Harding, 1998). The polymeric materials have lower shear wave velocity and lower density than the silicon dioxide, providing the potential for higher sensitivity, but devices incorporating polymers suffer from the disadvantage of having a higher acoustic loss. Both experimental work and modeling (McHale et al., 2001, 2002a,b) suggest that, for a particular polymer, the sensitivity to mass loading increases with the over-layer thickness and is optimum at the maximum slope of the dispersion curve. Quartz has a relatively small piezoelectric coupling coefficient and as a result considerable efforts have been made to produce Love-wave devices using materials with greater coupling such as lithium tantalate (LiTaO₃). Freudenberg et al. (2001) reported the use of a SiO₂ guiding layer on 36° rotated Y-cut X propagating lithium tantalate (36 YX.LT) and Barie et al. (1998) coated a LiTaO₃ device with a series of polymethylsiloxane co-polymers, resulting in reversible, reproducible signals and high long-term stability. Love-wave devices fabricated on a LiTaO₃ substrate have also been applied as biochemical sensors in liquid. Low level detection at high

* Corresponding author. Tel.: +44-115-8483365; fax: +44-115-8486636.

E-mail address: michael.newton@ntu.ac.uk (M.I. Newton).

frequency was achieved by Welsh et al. (1997) and, more recently, by Josse et al. (2001) and Bender et al. (2000) who investigated optimizing the sensitivity of Love-wave sensors with wave-guide thickness.

Surface skimming bulk waves (SSBW) and leaky SH-SAW both propagate on the 36° rotated Y-cut X propagating lithium tantalate (36 YX.LT) (Hashimoto, 2000). In this crystalline direction, the two modes exhibit a very close phase velocities with 4160 and 4212 ms^{-1} for the SSBW and leaky SH-SAW, respectively. The leaky SH-SAW mode is converted into a SSBW when the propagation surface is free, whereas it propagates as a leaky SH-SAW when the propagation surface is metallised. The SH-SAW that propagates on the metallised surface is affected by the mechanical properties of the adjacent liquid. However, a SH-SAW that propagates on a free surface is affected by both the mechanical and electrical properties of the adjacent liquid. In previous papers, we reported resonant conditions for guiding layer thickness on ST-Quartz (McHale et al., 2001) and also reported applications of these for biosensors (Newton et al., 2001a,b). In this paper, we extend this work to present experimental results for the discrimination of SSBW and leaky SH-SAW based Love waves and the application of a guided leaky SH-SAW to biosensing. The observation of fast dynamics of reactions requires the use of a fast interrogation system. Standard techniques employing continuous wave systems such as the network analyzer, measure the single transit signal, which may contain unwanted contributions from edge reflections and triple transit echoes. For the development of an improved arrangement for biosensing, it is useful to use a time-of-flight resolved information system in order to identify spurious reflections, discriminate between different acoustic modes and to aid the optimization of the sensitivity of devices. Examples of SH-SAW pulsed analysis have been already reported (Chung and McGill, 1998; Stevenson et al., 2001; Newton et al., 2001b). In this work, we extend the application of a pulse mode measurement system to utilize LiTaO_3 devices and give rapid amplitude and phase information for biosensing experiments.

2. Experimental

Delay line devices on 36 YX.LT were fabricated by using a standard photolithography process. Both the transmit and receive interdigital transducer (IDT) electrodes were of the same design and fabricated from sputtered Ti/Au of thickness $0.10 \mu\text{m}$. Each IDT consisted of 40 finger pairs with a period $\lambda = 45 \mu\text{m}$ and an aperture of 65λ . The basic SAW device supports the excitation of SSBW and leaky-type shear-horizontal modes with a center frequency f_0 at around 92 MHz and an insertion loss of approximately 22 dB . Guiding layers consisting of S1813 photoresist (Shipley Micro-Elec., Europe) were spun at 4000 rpm and cross-linked for 30 min at 160°C . A $0.10 \mu\text{m}$ layer, consisting of a Titanium flash and a Gold capping layer, was deposited on the path

length to discriminate the two modes excited by the IDT. A silicone gasket was used to isolate the SAW path from the IDT and liquid was passed through the flow cell at a rate of 5 ml min^{-1} . The experimental system used in this work uses a pulse excitation technique to monitor both amplitude and phase changes. The pulse mode system, previously reported for ST-Quartz Love-wave applications (Newton et al., 2001b), enables time-of-flight resolved information to be obtained and spurious reflections to be identified. The system used a continuous RF signal, which was power-split and one output fed to two cascaded double balance mixers combined with a pulse generator synchronized to an external clock source. This signal, which was effectively a short pulse of continuous wave, was then amplified and used to excite the input port of the SAW device. The output from the SAW was amplified, divided with a second power splitter and one output connected to a HP8471D diode detector; the output of the diode detector was then proportional to the amplitude. This signal was fed to one linear gate of a gated integrator and boxcar averager (Stanford Research Systems). The phase measurement used the other signals from the two power splitters. The first signal being a continuous RF signal and the second the pulsed output from the SAW device. These were fed to a third double balanced mixer set as a phase detector. The output of the phase detector included a dc component that, for the duration of the pulse, was proportional to the phase difference between the two inputs, which was fed to a second linear gate. The gated integrator and boxcar averager then provided continuously varying analogue outputs proportional to the amplitude and phase. The data capture rate was, therefore, constrained predominantly by the GPIB interface used to transfer data from the gated integrator and boxcar averager to the computer.

3. Results and discussion

By applying successive cross-linked S1813 photoresist polymer coatings on top of both a SSBW and leaky SH-SAW propagating on a 36 YX.LT device, we measured the minimum loss exhibited and the corresponding frequency of each mode. Previous work, which studied the effect of increasing the over-layer thickness on a SSBW device on ST-quartz (McHale et al., 2001), observed a series of resonance patterns in the insertion loss separated by a thickness consistent with a change of half an acoustic wavelength in the over-layer. In Fig. 1(a) and (b) we show the experimental results of the insertion loss change and resonant frequency shift with increasing polymer layers for the two 36 YX.LT modes. The Love-wave effect can be seen clearly for the SSBW mode (circles) with an initial reduction in the insertion loss and a reduction in frequency with increasing over-layer thickness. For thicker layers, the insertion loss increased rapidly and the frequency decreased with a sharp transition between 3 and $4 \mu\text{m}$. By further increasing the guiding layer thickness, resonance patterns in frequency and

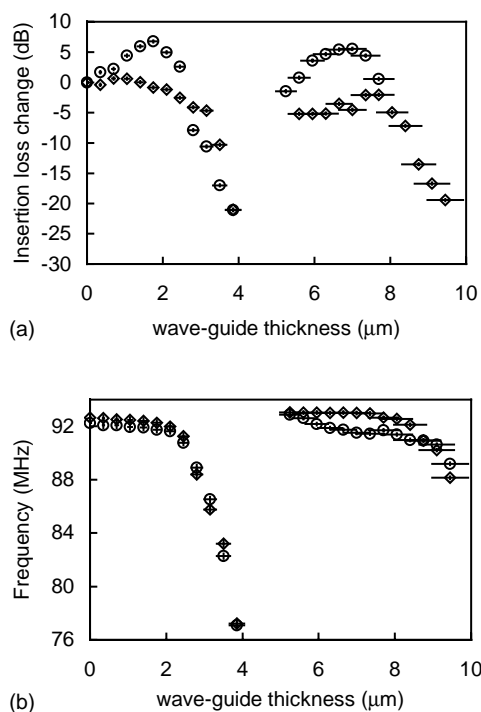


Fig. 1. Change in the: (a) insertion loss and (b) resonant frequency as a function of waveguide thickness for (\diamond) leaky SH-SAW and (\odot) SSBW on 36 YX.LT.

insertion loss are also observed. An identical process was applied to obtain the resonant conditions of leaky SH-SAW mode (diamonds). However, the leaky SH-SAW mode does not exhibit the initial decrease in insertion loss observed with the SSBW mode. For this mode, the insertion loss remains roughly constant before decreasing between 3 and 4 μm . The phase velocities of the leaky SH-SAW and SSBW modes on the 36 YX.LT have been predicted to be the same to within a few meters per second on the crystalline direction used in this work (Hashimoto, 2000). Indeed, up to 4 μm in Fig. 1(b) there is little difference between the leaky SH-SAW mode and the SSBW mode. However, at the greater thickness the two modes can be distinguished by a thin separation in operating frequency, showing that the leaky SH-SAW exhibits a slightly higher phase velocity than the SSBW when operating under thick guiding layers. The initially constant insertion loss with increasing guiding layer thickness of the guided leaky SH-SAW mode is consistent with Love-wave theory although the initial decrease in insertion loss of the guided SSBW is not predicted. The leaky SH-SAW and SSBW mode are both considered as shear waves, the key difference being in the propagation characteristics where the SSBW is launched at an angle of a few degrees to the surface and the leaky SH-SAW propagates parallel to the surface.

In Fig. 2, we show the changes (a) in phase and (b) in insertion loss of the non-metallised device to poly(ethylene glycol) (PEG) solutions with a molecular weight of 3350 for different values of overlayer thicknesses (d) using the following sequence (g l^{-1}): 80, 160, 240, 320, 400 and 480.

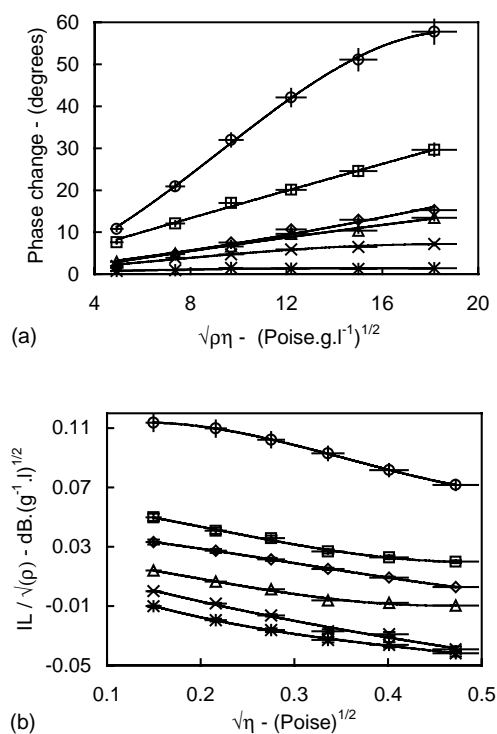


Fig. 2. (a) Change in phase vs. the square root of the solution density and viscosity product for SSBW propagation on 36 YX.LT, for increasing wave-guide thickness ((\odot) 0 μm , (\square) 0.35 μm , (\diamond) 1.05 μm , (Δ) 1.75 μm , (\times) 2.45 μm , to the square root of the density vs. the square root of the solution viscosity for the same range of wave-guide thickness.

These solutions were introduced to the device surface using a flow cell arrangement driven by a peristaltic pump; all changes in insertion loss and phase were made with respect to deionised water in the flow cell. As the phase velocity is density and viscosity dependent, phase changes are plotted as a function of the square root of the viscosity–density product $(\rho\eta)^{0.5}$, where ρ is the density of the solution and η the viscosity of the solution (Ricco and Martin, 1987). In Fig. 2(a), changes in phase remain positive and finally an asymptotic value is reached at $d = 13.15 \mu\text{m}$ at the highest $(\rho\eta)^{0.5}$ value. Following the same method as Ricco and Martin (1987), the way to illustrate the amplitude–viscosity relationship is by plotting the density-normalized insertion loss change as a function of the square root of the viscosity of the liquid. Changes in insertion loss produced by the solutions can be seen to be positive (lower insertion loss) but decrease with thicker guiding layers and finally become negative (greater insertion loss) for $d = 2.45 \mu\text{m}$ and above. The maximum change in insertion loss is observed for the uncoated device with a solution density of 80 g l^{-1} .

An identical liquid sensing procedure was used on the metallised device. In Fig. 3(a), we show the change in phase as a function of $(\rho\eta)^{0.5}$ for increasing wave-guide thickness. In contrast to the non-metallised device, values for phase change are all negative and significantly smaller in magnitude. Fig. 3(b) shows change in insertion loss normalized to

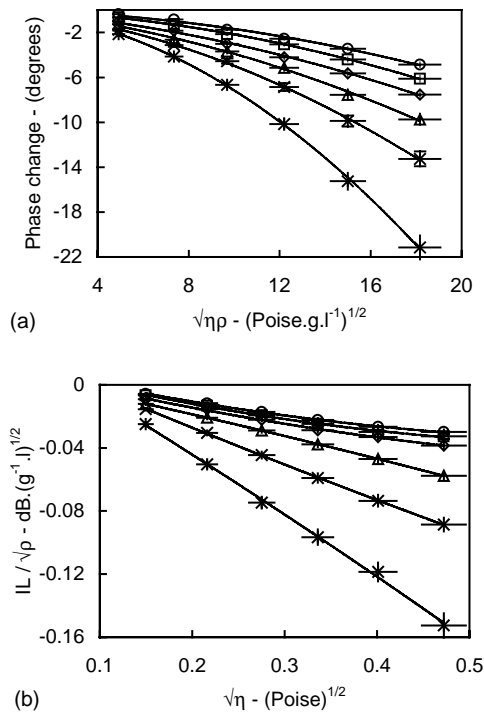


Fig. 3. (a) Change in phase vs. the square root of the solution density and viscosity product for leaky SH-SAW propagation on 36 YX.LT for increasing wave-guide thickness ((\odot): 0 μm , (\blacksquare) 0.35 μm , (\diamond) 1.05 μm , (\blacktriangle) 1.75 μm , (\times) 2.45 μm , (\star) 3.15 μm). (b) Change in insertion loss normalized to the square root of the density vs. the square root of the solution viscosity for the same range of wave-guide thickness.

the liquid density plotted as a function of the square root of the liquid viscosity for different values of overlayer thickness. In this figure, changes in insertion loss are now exclusively negative. Assuming that the liquid is in good contact with the polymer guiding layer so that non-slip condition is satisfied, acoustic energy will be coupled in the liquid layer. The penetration depth of a SH-SAW device when in contact with the liquid is $\delta = (2\eta/\rho\omega)^{0.5}$, where ω is the angular frequency. The penetration depth δ was calculated to vary between 82 and 284 nm for the range of solutions used.

As the viscosity increases, more energy is coupled into the liquid media so that the energy loss in Fig. 3(b) can be attributed to viscous dissipation into the liquid. Furthermore, Fig. 3(a) suggests that small variations of the viscosity of the solution will not affect the phase response of the Love-wave sensor when the guiding layer is thin. However, sensitivity to mass deposition increases with viscosity of the liquid layer, since more energy is coupled in viscous liquids.

Electrical interactions can occur between a surrounding liquid or an overlayer and the Love modes. Direct perturbation of the piezoelectric surface acoustic wave can occur due to acousto-electric effects. Quartz shows only weak coupling and the guiding layer provides an electrical shielding, so this effect can be negligible. However, lithium tantalate exhibits a very high coupling and the SH-SAW that propagates on the surface of 36 YX.LT has an electric field that

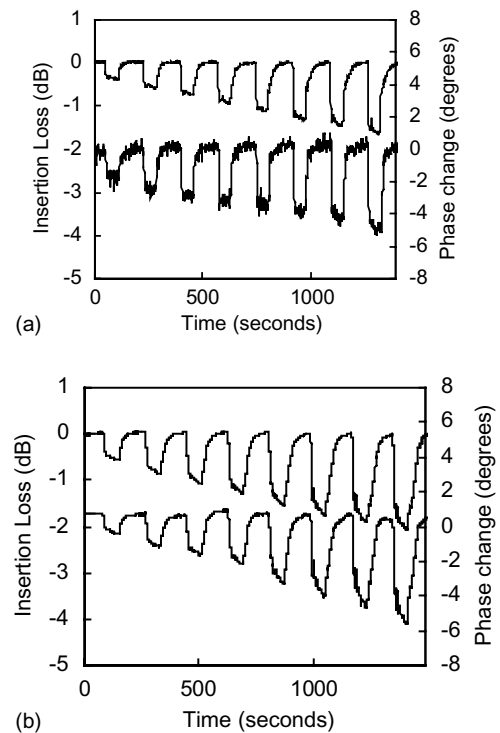


Fig. 4. Change in insertion loss (upper line) and in phase (lower line) for a sequence of different concentrations of 3350 molecular weight poly(ethylene glycol) solutions using: (a) the continuous wave system and (b) the pulse mode system.

extends several microns into the adjacent liquid (Kondoh and Shiokawa, 1993). In Fig. 2(a), at approximately $d = 3.15 \mu\text{m}$ an asymptotic value of phase is reached. Changes in loss become systematically negative at $d = 2.45 \mu\text{m}$ in Fig. 2(b). This means that the layer is sufficiently thick such that all the electric field is concentrated in the guiding layer and substrate. Hence, viscous liquid loading takes place and surface impedance changes are predominantly due to viscous coupling.

Using a 1 μm polymer guiding layer on a leaky SH-SAW device we investigated the effect of a lipid monolayer using both a continuous wave (CW) system and pulse mode system. To provide a simple calibration for the pulse mode system prior to the biosensing experiments, an experiment was devised using different concentrations of 3350 molecular weight poly(ethylene glycol) (PEG) in the following sequence (g l^{-1}): 34.4, 68.8, 13.2, 137.6, 172.0, 206.4, 240.8, 275.2. Fig. 4(a) and (b), respectively, shows the CW system and the pulse mode amplitude and phase measurements for this sequence. The PEG solutions and deionised water were alternately pumped over the device surface. The initial baseline signal with deionised water changed rapidly when replaced by the PEG solutions. When deionised water is once again pumped over the device surface, the signal returns to its original value, showing that the PEG is fully removed.

This sequence was repeated many times and shown to produce repeatable changes to within 5% in phase and

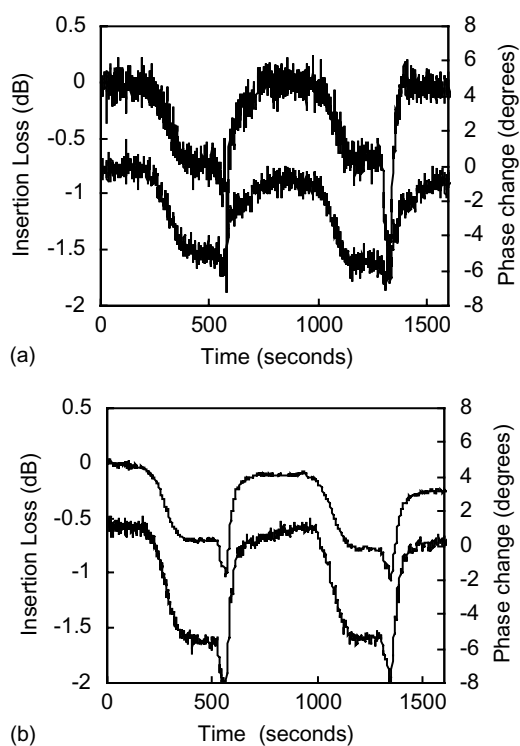


Fig. 5. Change in insertion loss (upper line) and in phase (lower line) for two cycles of deposition and removal of POPC by using: (a) the network analyzer and (b) the pulse mode system.

amplitude using the pulse mode system and the continuous mode system. A LeCroy 9362C 1.5 GHz bandwidth oscilloscope and a set of calibrated attenuators were used to further verify the magnitude of the changes in amplitude and phase for the two systems. The two methods were found to be in agreement to within 10%. The SH-SAW device was subsequently made hydrophilic by treatment with a sol-gel derived silica coating. Hydrochloric acid was used to accelerate and polymerize a silica solution. The gel was placed on the guiding layer surface, left for 2 min and rinsed off with water. In Fig. 5(a), we show the change in insertion loss and phase as a function of time for a model biosensing experiment with the CW system. The device was initially immersed into a buffer solution, phosphate buffered saline (PBS), which was then followed, at $t = 125$ s, by the deposition of 0.2 mg ml^{-1} of vesicles of palmitoyl-oleoyl-*sn*-glycerophosphocholine (POPC) in PBS. The vesicle layer was then removed at $t = 475$ s, by a detergent, *t*-octyl-phenoxy-poly(ethoxyethanol) (Triton) at 0.1% (v/v) in PBS. The signal is observed to return to its original value, indicating that the POPC was readily rinsed off. It was followed by a second sequence of POPC deposition at $t = 875$ s and removal at $t = 1250$ s. The rapid transition in insertion loss and phase is typical of the POPC removal process as the addition of detergent disrupts the adsorbed vesicles and has been already reported (Melzak and Gizeli, 2002). The hydrophilic surface preparation presents a rough surface, which induces absorption of vesicle layer

resulting in a large signal change, which is expected for the formation of a viscoelastic layer. Fig. 5(b) shows the equivalent experiment using the pulse mode system; in this case, the first deposition of POPC in PBS was at $t = 100$ s and then removed at $t = 400$ s and was followed by a second sequence of POPC deposition at $t = 850$ s and removal at $t = 1250$ s. The sampling rate of the pulse mode system was chosen to be 86 measurements per minute in common with the CW system, although the maximum sampling rate of the pulse mode system is much faster but limited by the GPIB transfer rate; the use of a fast A/D converter would allow several hundreds measurements to be made each minute.

4. Conclusion

In this paper, we have shown that two SH-SAW modes can be excited on 36 YX.LT substrates, discriminated and converted into two distinctive wave-guided modes. Furthermore, the idea of mode distinction was applied to liquid sensing and metallising the sensing area was found to efficiently eliminate acousto-electric effects. To achieve higher sensitivity in phase and insertion loss for liquid sensing, the waveguide thickness of the polymer was increased. A relatively strong Love wave with a relatively low insertion loss, re-occurred as the guiding layer was increased, corresponding to higher order mode Love-wave mode. Mass sensitivity of such higher order modes is lower than the first Love-wave mode by factor of 2 or 3 only (McHale et al., 2002a). This suggests that it should be possible to use relatively thick wave-guiding layers without completely sacrificing to mass sensitivity and, hence, extend the range of wave-guide materials that can be used with layer guided acoustic sensors. Molecularly imprinted polymer materials (MIP) show potential for sensitising layers on acoustic wave devices (Percival et al., 2001, 2002). However, to the authors knowledge, there have been no reports of techniques for fabricating MIP films of controlled thickness in the range $0.1\text{--}5 \mu\text{m}$ required for operating in the first Love mode. Jakoby et al. (1999) showed it is possible to fabricate a MIP hybrid Love-wave device for gas sensing by initially extending the SiO_2 wave-guide thickness, whereas Love-wave operation at the second or third Love mode would allow the MIP layer to directly be used as a potential wave-guide.

Acknowledgements

The authors gratefully acknowledge the financial support of BBSRC provided by research Grant E11140.

References

- Barie, N., Rapp, M., Ache, H.J., 1998. UV crosslinked polysiloxanes as new coating material for SAW devices with high long term stability. *Sens. Actuators B* 46, 97–103.

- Bender, F., Cernosek, R.W., Josse, F., 2000. Love-wave biosensors using cross-linked polymer waveguides on LiTaO₃ substrates. *Electr. Lett.* 36, 1672–1673.
- Chung, R., McGill, R.A., 1998. Performance of a polymer coated SAW device under pulse excitation. *IEEE Inter. Freq. Contr. Symp.* 634–638.
- Du, J., Harding, G.L., 1998. A multiplayer structure for Love-mode acoustic sensors. *Sens. Actuators A* 65, 152–159.
- Freudenberg, J., Von Schickfus, M., Hunklinger, S., 2001. A SAW immunosensor for operation in liquid using a SiO₂ protective layer. *Sens. Actuators B* 76, 147–151.
- Gizeli, E., Stevenson, A.C., Goddard, N.L., Lowe, C.R., 1992. A novel Love-plate acoustic sensor utilizing polymer overlayers. *IEEE Trans. Ultrason. Ferroelectr. Freq. Control* 39, 657–659.
- Gulyaev, Y.V., 1998. Review of shear surface acoustic waves in solids. *IEEE Trans. Ultrason. Ferroelectr. Freq. Control* 45, 935–938.
- Harding, L.G., Du, J., 1997. Design and properties of quartz-based Love-wave acoustic sensors incorporating silicon dioxide and PMMA guiding layers. *Smart Mater. Struct.* 6, 716–720.
- Hashimoto, K.Y., 2000. Surface acoustic wave devices for telecommunications. *Modeling and Simulation*. Springer-Verlag, ISBN 3-540-67232-X.
- Jakoby, B., Vellekoop, M.J., 1998. Analysis and optimisation of Love-wave liquid sensors. *Ferroelectr. Freq. Control* 45, 1293–1301.
- Jakoby, B., Ismael, G.M., Byfield, M.P., Vellekoop, M.J., 1999. A novel molecularly thin film applied to a Love-wave gas sensor. *Sens. Actuators A* 65, 93–97.
- Josse, F., Bender, F., Cernosek, R.W., 2001. Guided shear horizontal-surface acoustic wave sensors for chemical and biochemical detection in liquids. *Anal. Chem.* 73, 5937–5944.
- Kondoh, J., Shiokawa, S., 1993. A shear-horizontal SAW device as a pH monitor. *Sens. Actuators B* 13, 429–431.
- Kovacs, G., Vellekoop, M.J., Haueis, R., Lubking, G.W., Venema, A., 1994. A Love sensor for (bio)chemical sensing in liquids. *Sens. Actuators A* 43, 38–43.
- McHale, G., Newton, M.I., Martin, F., 2001. Resonant conditions for Love-wave guiding layer thickness. *Appl. Phys. Lett.* 79, 3542–3543.
- McHale, G., Newton, M.I., Martin, F., 2002a. Theoretical mass sensitivity of Love-wave and layer guided acoustic plate mode sensors. *J. Appl. Phys.* 91, 9701–9710.
- McHale, G., Newton, M.I., Martin, F., 2002b. Layer guided shear horizontally polarized acoustic plate modes. *J. Appl. Phys.* 91, 5735–5744.
- Melzak, K.A., Gizeli, E., 2002. A silicate gel promoting deposition of lipid bilayers. *J. Colloid Interface Sci.* 246, 21–28.
- Newton, M.I., Martin, F., Melzak, K., McHale, G., 2001a. Harmonic Love-wave devices for biosensing applications. *Electr. Lett.* 37 (6), 340–341.
- Newton, M.I., McHale, G., Martin, F., Gizeli, E., Melzak, K., 2001b. Pulse mode operation of Love-wave devices for biosensing applications. *Analyst* 126, 2107–2109.
- Percival, C.J., Stanley, S., Galle, M., Braithwaite, A., Newton, M.I., McHale, G., Hayes, W., 2001. Molecular imprinted polymer coated quartz crystal microbalances for the detection of terpenes. *Anal. Chem.* 73, 4225–4228.
- Percival, C.J., Stanley, S., Braithwaite, A., Newton, M.I., McHale, G., 2002. Molecular imprinted polymer coated acoustic wave devices for the detection of Nandrolone. *Analyst* 127, 1024–1026.
- Ricco, A.J., Martin, S.J., 1987. Acoustic wave viscosity sensor. *Appl. Phys. Lett.* 50 (21), 1474–1476.
- Stevenson, A., Mehta, H., Sehti, R., Cheran, L.-E., Thompson, M., Davies, I., Lowe, C.R., 2001. Gigahertz surface acoustic wave probe for chemical analysis. *Analyst* 126, 1619–1627.
- Welsh, W., Klein, C., Oksuzoglu, R.M., Von Schickfus, M., Hunklinger, S., 1997. Immunosensing with surface acoustic wave sensors. *Sens. Actuators A* 62, 562–564.